lations indicate that if the Reynolds number for transition is based on local Reynolds number and x at the disturbance origin, transition Reynolds number is weakly dependent on hypersonic Mach number for $M_e > 7$.

Together with the lateral spreading angle information, the wall spreading angle data makes it possible to construct simplified cross sections of three-dimensional turbulent disturbance growth behavior. Side and frontal views of these simplified cross sections are presented in Fig. 2 for three local Mach numbers; $M_e = 0$, $M_e = 3$, and $M_e = 14$. The varying nature of turbulence growth (based on Fig. 1) as a function of Mach number is evident. For the $M_e = 14$ case, the outer transitional growth which occurs far upstream of the wall transition location provides a plausible explanation for the observed increase[1,24] in experimental boundary-layer thicknesses (above the theoretical laminar value) upstream of transition. The visualization of turbulence growth and development presented herein may be of interest to the predictors who need to model transition in order to develop numerical techniques for transitional flow regions.

References

[1] Fischer, M. C. and Weinstein, L. M., "Cone Transitional Boundary-Layer Structure at $M_e = 14$," *AIAA Journal*, Vol. 10, No. 5, May 1972, pp. 699–701.

[2] Staylor, W. F. and Morrisette, E. L., "Use of Moderate-Length Hot-Wires to Survey a Hypersonic Boundary Layer," *AIAA Journal*, Vol. 5, No. 9, Sept. 1967, pp. 1698–1700.

[3] Potter, J. L. and Whitfield, J. D., "Effects of Slight Nose Bluntness and Roughness on Boundary-Layer Transition in Supersonic Flow," *Journal of Fluid Mechanics*, Vol. 12, 1962, pp. 501–535.

[4] Maddalon, D. V. and Henderson, A. Jr., "Boundary-Layer Transition on Sharp Cones at Hypersonic Mach Numbers," *AIAA Journal*, Vol. 6, No. 3, March 1968, pp. 424–431.

[5] Schubauer, G. B. and Klebanoff, P. S., "Contributions on the Mechanics of Boundary-Layer Transition," Rept. 1289, 1956, NACA.

[6] Charters, A. C. Jr., "Transition Between Laminar and Turbulent Flow by Transverse Contamination," TN 891, 1943, NACA.

[7] LaGraff, J. E., "Observations of Boundary-Layer Transition in Mach 7 Gun Tunnel with a Hot-Wire Anemometer," AIAA Paper 71-199, New York, 1971.

[8] Liepmann, H. W., Roshko, A., and Ohawan, S., "On the Reflection of Shock Waves from Boundary Layers," TN 2334, April 1951, NACA.

[9] Hicks, R. M. and Harper, W. R. Jr., "A Comparison of Spherical and Triangular Boundary Layer Trips on a Flat Plate at Supersonic Speeds," TM X-2146, Dec. 1970, NASA.

[10] Stalder, J. R. and Slack, E. G., "The Use of a Luminescent Lacquer for the Visual Indication of Boundary Layer Transition," TN-2263, Jan. 1951, NACA.

[11] Stone, D. R. and Cary, A. M. Jr., "Discrete Sonic Jets Used as Boundary Layer Trips at Mach Numbers of 6 and 8.5," Prospective TN D-(L-8215), 1972, NASA.

[12] Korkegi, R. H., "Transition Studies and Skin Friction Measurements on an Insulated Flat Plate at a Mach Number of 5.8," *Journal of the Aeronautical Sciences*, Vol. 23, No. 2, Feb. 1956, pp. 97–107, 192.

[13] Klebanoff, P. S. and Tidstrom, K. D., "Evolution of Amplified Waves Leading to Transition in a Boundary Layer with Zero Pressure Gradient," TN D-195, Sept. 1959, NASA.

[14] Wagner, R. D. Jr., Maddalon, D. V., and Weinstein, L. M., "Influence of Measured Free Stream Disturbances in Hypersonic Boundary Layer Transition," *AIAA Journal*, Vol. 8, No. 9, Sept. 1970, pp. 1664–1670.

[15] Whitehead, A. H. Jr., "Flow-Field and Drag Characteristics of Several Boundary Layer Tripping Elements in Hypersonic Flow," TN D-5454, Oct. 1969, NASA.

[16] Mitchner, M., "Propagation of Turbulence from an Instantaneous Point Disturbance," *Readers' Forum, Journal of the Aeronautical Sciences*, Vol. 21, No. 5, May 1954, pp. 350–351.

[17] Van Driest, E. R. and McCauley, W. D., "The Effect of Controlled Three-Dimensional Roughness on Boundary-Layer Transition at Supersonic Speeds," *Journal of the Aerospace Sciences*, April 1960, pp. 261–271, 303.

[18] Loving, D. L. and Katzoff, S., "The Fluorescent Oil Film Method and Other Techniques for Boundary Layer Flow Visualization," Memo 3-17-59 L, March 1959, NASA.

[19] Fischer, M. C., "An Experimental Investigation of Boundary Layer Transition on a 10° Half-Angle Cone at Mach 6.9," TN D-5766, April 1970, NASA.

[20] Owen, F. K., "Fluctuation and Transition Measurements in Compressible Boundary Layers," AIAA Paper 70-745, Los Angeles, Calif., 1970.

[21] Hastings, R. C. and Sawyer, W. G., "Turbulent Boundary Layers on a Large Flat Plate at $M = 4$," TR 70040, March 1970, Royal Aircraft Establishment, Bedford, England.

[22] Stainback, P. C., "Use of Rouse's Stability Parameter in Determining the Critical Layer Height of a Laminar Boundary Layer," *AIAA Journal*, Vol. 8, No. 1, Jan. 1970, pp. 173–175.

[23] Channapragada, R. S., "A Compressible Jet Spread Parameter for Mixing Zone Analysis," TM-14-63-U25, May 1963, United Technology Center.

[24] Fischer, M. C. and Maddalon, D. V., "Experimental Laminar, Transitional, and Turbulent Boundary Layer Profiles on a Wedge at Local Mach Number 6.5 and Comparisons with Theory," TN D-6462, Sept. 1971, NASA.

Reflection of Weak Shock Waves from Permeable Materials

G. S. BEAVERS* AND R. K. MATTA†

University of Minnesota, Minneapolis, Minn.

Introduction

In recent years considerable attention has been given to the use of permeable materials as sound attenuating devices, with particular interest concerned with the attenuating effects of the permeable material on the reflected and transmitted sound waves. Similarly, when a weak shock wave strikes a plane surface and is reflected, the strength of the reflected wave is lower when the reflecting surface is permeable than when the surface is impermeable. There appears, however, to be very little information available on the attenuation of shock waves reflected from permeable surfaces, although recently Cloutier and co-workers[1] have reported some observations on the attenuation of weak oblique shocks by porous surfaces. In this Note, we present some experimental observations which show the attenuating effects of three different permeable materials on the reflected shock strength. A simple analytical model is presented which consists essentially of the coupled problems of the reflection of a plane shock wave and the steady, compressible flow through a permeable material.

The flow configuration (Fig. 1) consists of a plug of permeable material positioned in a duct of constant cross-sectional shape. For this work, a permeable material is defined as a solid medium containing a large number of interconnected pores which are dispersed throughout the material in a random manner. The initial state is everywhere uniform, and the volume downstream of the permeable plug is very large, so that the pressure downstream of the material is assumed to remain constant. A plane shock wave strikes the front face of the permeable plug, and is reflected. The increased pressure thus formed at the front face of the plug creates a flow through the material. It is assumed that the material is sufficiently dense so that there is no transmitted

Received January 17, 1972; revision received February 23, 1972. This work was supported in part by the National Science Foundation under Grant GK 13303 and by the Department of Defense under Grant N00014-68-A-0141-0001 administered by the Office of Naval Research.

Index category: Shock Waves and Detonations.

* Associate Professor, Department of Aerospace Engineering and Mechanics. Member AIAA.

† Research Fellow, Department of Aerospace Engineering and Mechanics.

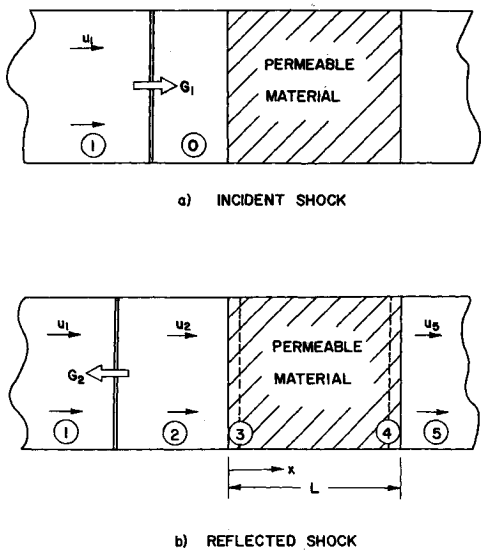

Fig. 1 Flow configuration and notation.

shock. Further, in the analytical model it is assumed that any transient effects, which may occur immediately after the shock reflection, have decayed so that the reflected shock is traveling with constant velocity and the flow through the permeable material is steady.

Analytical Model

It is required to calculate the reflected shock velocity for a given incident velocity and known properties of the permeable material. For this model, air is treated as a perfect gas ($\gamma = 1.4$) and the variation of viscosity with temperature is neglected.

We consider first the flow through the permeable material, the analysis of which parallels that given in Ref. 2. It has been pointed out[2,3] that a complete description of this flow must include a description of the flow entering and leaving the material, where the flow experiences sudden area changes. To do this the flow region is divided into three parts, as shown in Fig. 1. States 2 and 5 correspond, respectively, to locations immediately upstream and downstream of the permeable plug. State 3 describes the gas within the plug just downstream of the front face, and state 4 describes the gas just within the plug at the downstream end. The gas adjusts from state 2 to state 3 and from state 4 to state 5 in a distance of a few pore diameters, which is negligible compared with the over-all length of the plug. Thus, distances in the streamwise direction for the main body of the material can be measured from the front face with negligible error.

For the flow through the main body of the permeable plug (3 to 4), it has been argued[2] that, by making use of the extended Darcy law,[4] the appropriate form of the momentum equation is

$$\rho u\, du/dx = -dp/dx - \{(\varepsilon\mu/k)u + [c\varepsilon^2/(k)^{1/2}]\rho u^2\} \quad (1)$$

where u is the mean gas velocity through the pore space at any cross section, ε is the porosity, k is the permeability, and c is a constant which appears in the nonlinear extension to the Darcy law and which depends on the particular class of permeable materials under consideration. The continuity equation within the plug can be expressed as

$$Q = \rho u = \text{const} \quad (2)$$

Making the assumption of no heat transfer at the outer bounding walls of the permeable plug, and using the gas law, Eq. (1) can be integrated across the thickness L of the plug to give

$$2\gamma DL/(k)^{1/2} = F(M_3^2) - F(M_4^2) \quad (3)$$

where

$$F(M^2) = 1/M^2 + \tfrac{1}{2}(\gamma+1)\ln\{M^2/[1+\tfrac{1}{2}(\gamma-1)M^2]\} \quad (4)$$

and the constant D is given by

$$D = c\varepsilon^2 + \mu\varepsilon/Q(k)^{1/2} \quad (5)$$

Further, the pressures at states 3 and 4 are related by

$$(p_4/p_3)^2 = M_3^2[1+\tfrac{1}{2}(\gamma-1)M_3^2]/M_4^2[1+\tfrac{1}{2}(\gamma-1)M_4^2] \quad (6)$$

We now consider the flow in the entry and exit regions of the plug. Emanuel and Jones[3] argued that the flow between states 2 and 3 is analogous to that in a converging nozzle, with the gas undergoing an isentropic expansion. It follows[2,3] that the Mach numbers are related by

$$\varepsilon^2 M_3^2/M_2^2 = \{[1+\tfrac{1}{2}(\gamma-1)M_3^2]/[1+\tfrac{1}{2}(\gamma-1)M_2^2]\}^{(\gamma+1)/(\gamma-1)} \quad (7)$$

and the pressures by

$$p_3/p_2 = (M_2/\varepsilon M_3)^{2\gamma/(\gamma+1)} \quad (8)$$

In describing the flow out of the plug, Emanuel and Jones[3] suggested that the flow experiences a sudden area change, which is an adiabatic but nonisentropic process, and the appropriate momentum equation is then

$$(1-\varepsilon)p_4 + \varepsilon(p_4 + \rho_4 u_4^2) = p_5 + \rho_5 u_5^2$$

From this equation the pressure ratio is derived as

$$p_5/p_4 = (1+\varepsilon\gamma M_4^2)/(1+\gamma M_5^2) \quad (9)$$

Finally, we note that the whole process from 2 to 5 is adiabatic, so that

$$(p_5/p_2)^2 = M_2^2[1+\tfrac{1}{2}(\gamma-1)M_2^2]/M_5^2[1+\tfrac{1}{2}(\gamma-1)M_5^2] \quad (10)$$

Then, using Eqs. (6–10), the Mach numbers at states 4 and 5 can be related in the form

$$\varepsilon^2 M_4^2[1+\tfrac{1}{2}(\gamma-1)M_4^2]/(1+\varepsilon\gamma M_4^2)^2 = M_5^2[1+\tfrac{1}{2}(\gamma-1)M_5^2]/(1+\gamma M_5^2)^2 \quad (11)$$

We now consider the shock reflection process, noting that there is a nonzero gas velocity behind the reflected shock. It is convenient to work in terms of velocities made dimensionless by the speed of sound, a_0, in the initial undisturbed gas, and also to use the speed of sound ratios as intermediate computational para-

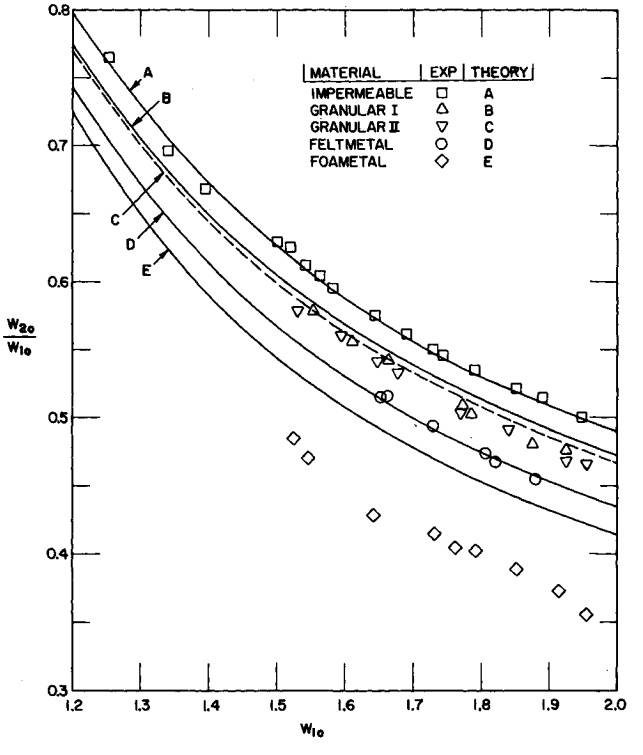

Fig. 2 Dependence of reflected shock speed on incident speed and material parameters.

meters. The following results may then be derived for the incident shock, using the notation given in Fig. 1:

$$U_{10} = 2(W_{10}^2 - 1)/(\gamma+1)W_{10} \quad (12)$$

$$p_1/p_0 = [2\gamma W_{10}^2 - \gamma + 1]/(\gamma+1) \quad (13)$$

$$A_{10}^2 = [2\gamma W_{10}^2 - \gamma + 1][(\gamma-1)W_{10}^2 + 2]/(\gamma+1)^2 W_{10}^2 \quad (14)$$

where

$$W_{10} = G_1/a_0, \quad U_{10} = u_1/a_0, \quad A_{10} = a_1/a_0, \quad W_{20} = G_2/a_0$$

The pressure ratio across the reflected shock can be obtained as

$$p_2/p_1 = [2\gamma(U_{10}+W_{20})^2 - (\gamma-1)A_{10}^2]/(\gamma+1)A_{10}^2 \quad (15)$$

and the Mach number of the gas behind the reflected shock is

$$M_2 = \left[\frac{(\gamma-1)(U_{10}+W_{20})^2 + 2A_{10}^2}{2\gamma(U_{10}+W_{20})^2 - (\gamma-1)A_{10}^2}\right]^{1/2} - \frac{W_{20}}{A_{20}} \quad (16)$$

where

$$A_{20}^2 = \frac{[2\gamma(U_{10}+W_{20})^2 - (\gamma-1)A_{10}^2][(\gamma-1)(U_{10}+W_{20})^2 + 2A_{10}^2]}{(\gamma+1)^2(U_{10}+W_{20})^2} \quad (17)$$

Finally, from considerations of mass conservation across the reflected shock, an expression involving the quantity Q of Eq. (2) can be obtained:

$$\frac{\varepsilon Q}{\rho_0 a_0} = \left[\frac{W_{10}}{W_{10}-U_{10}}\right]\left\{U_{10} + W_{20}\left[\frac{A_{10}^2 - (U_{10}+W_{20})^2}{A_{10}^2 + \frac{1}{2}(\gamma-1)(U_{10}+W_{20})^2}\right]\right\} \quad (18)$$

When the initial state of the gas and the characteristics of the permeable material are specified, the above equations can be solved by a simple numerical procedure to yield W_{20} as a function of W_{10}. The computation makes use of the fact that $p_5 = p_2$, and allowance is made for the possibility of choking at state 4.

Experiments

The experiments were carried out in a conventional diaphragm shock tube of 3-in. × 3-in. cross section, using air as the working medium. Three different types of permeable material were used, classified as Foametal, Feltmetal and granular. Foametal consists of a latticework of metallic fibres such that there are no free fibre ends within the material, whereas Feltmetal consists of short sintered fibres with free ends of fibres lying within the material. The properties of these materials were taken from earlier experiments,[4] and are listed in Table 1. The granular material consisted of aluminum oxide grains of uniform size held together with a ceramic bond. The values of ε and k were known from earlier work, and a value for c was deduced from experimental results on the flow through beds of polyethylene particles. The surface of the permeable plugs which faced the incident shock was machined flat, so that the resulting surface consisted of a flat plane with a large number of pores penetrating into the material.

Results

Initial-experiments were performed using a smooth flat impermeable wall as a reflecting surface, with a range of incident shock Mach numbers chosen to correspond to the range used in the experiments with the permeable plugs. All incident and reflected shock speeds were obtained by timing over distances of a few inches. The speeds were checked at several distances from the plug and found to be closely constant. The measured reflected shock speeds are compared with calculated values in Fig. 2, where the calculated curve is that for air with the vibrational energy included. Figure 2 also compares the experimentally determined reflected shock speeds from the permeable plugs with the computed values. It is seen that the analytical model agrees fairly well with the experiments, except for the Foametal plug. There are two possible reasons for this discrepancy: 1) the material is exceedingly porous so that a transmitted shock may have occurred and 2) the material tended to exhibit some distortion after several shock reflections, so that the plug had to be changed periodically. However, it would appear from the other results that the analytical model gives a reasonable prediction of the reflected shock speeds for permeable materials which have porosity values such that transmitted shocks do not occur.

Table 1 Properties of permeable plugs

Material	L, in.	ε	k, in.$^2 \times 10^6$	c
Foametal	1.0	0.95	15.0	0.075
Feltmetal	0.25	0.80	0.8	0.132
Granular I	1.0	0.35	1.0	0.26
Granular II	1.0	0.35	2.5	0.26

References

[1] Cloutier, M., Devereaux, F., Doyon, P., Fitchett, A., Heckman, D., Moir, L., and Tordif, L., "Reflections of Weak Shock Waves from Acoustic Materials," *Journal of the Acoustical Society of America*, Vol. 50, No. 5, Nov. 1971, pp. 1393–1396.

[2] Beavers, G. S. and Sparrow, E. M., "Compressible Gas Flow Through a Porous Material," *International Journal of Heat and Mass Transfer*, Vol. 14, No. 11, Nov. 1971, pp. 1855–1859.

[3] Emanuel, G. and Jones, J. P., "Compressible Gas Flow Through a Porous Plate," *International Journal of Heat and Mass Transfer*, Vol. 11, No. 5, May 1968, pp. 827–836.

[4] Beavers, G. S. and Sparrow, E. M., "Non-Darcy Flow Through Fibrous Porous Media," *Journal of Applied Mechanics*, Vol. 36, No. 4, Dec. 1969, pp. 711–714.

Unified Area Rule for Hypersonic and Supersonic Wing-Bodies

W. H. Hui*

University of Waterloo, Ontario, Canada

FOR low supersonic flow there exists the well-known area rule by which the effect of wing-body interference on over-all forces can be obtained without a knowledge of the details of the local flowfield for a wide class of practically interesting configurations. In the hypersonic range an analogous theorem was given by Ladyzhenskii[1] for the wave drag of blunted-nose bodies at zero incidence. The lifting case was recently studied by Malmuth[2] who derived a new area rule for the change in the aerodynamic efficiency L/D of a hypersonic delta wing due to the addition on its compression side of a conical body of arbitrary shape. However, his analysis is restricted to hypersonic flow past wing-body configurations at small incidence. Furthermore, the conically subsonic flow region, on which the conical body is added, is assumed a small portion of the wing. There is obviously a Mach number range for which neither the supersonic area rule nor Malmuth's hypersonic area rule can be applied.

On the other hand, a unified theory for flow past delta wings was given by the author[3] which is valid for both hypersonic and supersonic flow past delta wings of any sweep angle at any incidence, provided the shock wave is attached to the leading edges. It gives almost identical results compared with large scale numerical solutions. The purpose of this paper is to show, by combining the methods of Refs. 2 and 3, that all the restrictions

Received January 24, 1972.

* Assistant Professor, Department of Applied Mathematics, on leave from Department of Aeronautics and Astronautics, University of Southampton, England.